

Microstructure and Wear Resistance in Medium and High C Steels Treated by Quenching and Partitioning

Eider Del Molino,* Maribel Arribas, Iñaki Pérez, Félix Valdavidia,
and Javier Jesús González

The quenching and partitioning (Q&P) steels have shown to be promising candidates to be applied in fields where wear resistance is required. In this study, a medium and a high C steel are heat treated by Q&P and the resulting microstructure, hardness, and wear resistance are characterized. The mechanical stability of the austenite phase under wear test conditions is investigated. It is found that the stability of austenite is very high in the high C steel and decreases in the medium C steel. Additionally, the hardness and wear behavior of the Q&P-treated steels are compared with the results obtained for quenching and tempering (Q&T) treated samples, showing that, although the hardness of Q&P steels is quite lower, the obtained wear rates are similar. It means that in the studied Q&P steels, although the austenite transformation into martensite does not occur considerably, the presence of austenite might play a key role in the wear resistance.

Therefore, other methods are being investigated to increase the wear resistance of steels without drastic loss of other important properties.

The quenched and tempered (Q&T) steels are quite hard and show good wear performance. However, some studies demonstrated that microstructures containing retained austenite (RA), despite having lower hardness, presented better wear resistance.^[3,5–7] RA is a relatively soft phase compared to martensite. Thus, the hardness of steel is primarily determined by the amount of martensite present, so as the content of RA increases, the hardness of the steel decreases.^[8] In addition, the more C enriched the austenite, the more depleted is the martensite; hence, lower

is the hardness of the matrix.^[9] Regarding RA in wear applications, one of the mechanisms proposed to explain the role of RA in quenching and partitioning (Q&P) steels includes that under mechanical loading, a higher amount of RA helps to obtain a thicker hardened layer due to its transformation into martensite. Other proposed mechanism is that a certain volume fraction of RA can absorb part of energy under high load, mitigating damage to the matrix.^[10]

More recently, Q&P-treated steels have been studied in a wear context and have shown to be of interest for wear applications. In the Q&P treatment, the steel is first quenched to a temperature between the martensite start (M_s) and the martensite finish (M_f) temperatures, the so-called quenching temperature (QT), followed by a partitioning treatment applied at a given partitioning temperature (PT) and during a given partitioning time (Pt). The partitioning stage is designed to enrich the remaining untransformed austenite with C that escapes from the martensite phase. This thermal treatment results in a martensitic microstructure with significant content of RA,^[11,12] which depends on the steel chemical composition and the heat treatment parameters. The addition of certain alloying elements is required in Q&P steels to suppress competing reactions that may occur during partitioning, such as carbide precipitation and decomposition of austenite. Commonly, Si is employed to suppress carbide formation and Mn to reduce bainite formation.^[13,14]

Most of the studies related to Q&P benefits for wear resistance correspond to the mining industry.^[15–18] In general, it is concluded that the RA is very beneficial for the tribological behavior (wear and friction). Consequently, in Q&P steels, apart from the direct relationship between hardness and wear resistance, the latter also depends on the microstructure and, therefore, on


1. Introduction

Wear resistance is directly related with the service life and performance of the components and, therefore, significant research effort has been made to improve wear resistance of the materials. Typically, the wear resistance of steels is directly related with hardness, although many other factors must be considered, such as microstructure.^[1–3] Increased hardness is generally obtained by increasing the C content of the steel. However, the higher C content typically leads to a decrease in other properties of interest, such as toughness, bendability, and weldability.^[4]

E. Del Molino, M. Arribas, I. Pérez
Tecnalia, Basque Research and Technology Alliance (BRTA)
Parque Científico y Tecnológico de Bizkaia, Astondo Bidea, 700, E-48160
Derio, Spain
E-mail: eider.delmolino@tecnalia.com

F. Valdavidia
Alfe Cutting
Polígono Bildosola, Parcela B2, E-48412 Artea, Spain

J. J. González
Department of Mining and Metallurgical Engineering
University of the Basque Country (ETSI Bilbao UPV/EHU)
Calle Alameda Urquijo s/n, 48013 Bilbao, Spain

 The ORCID identification number(s) for the author(s) of this article can be found under <https://doi.org/10.1002/srin.202300056>.

© 2023 The Authors. Steel Research International published by Wiley-VCH GmbH. This is an open access article under the terms of the Creative Commons Attribution License, which permits use, distribution and reproduction in any medium, provided the original work is properly cited.

DOI: 10.1002/srin.202300056

the Q&P process conditions (QT, PT, Pt).^[15] Although the C content of the austenite can be of greater importance than the austenite content against wear,^[19] generally, higher austenite content is translated into better abrasive wear performance.

A clear example of this phenomenon is shown in the work of Wasiak et al.,^[16] who observed that wear is reduced by practically 50% in the case of Q&P compared to Q&T in a 35CrSiMn5-5-4 steel. P. Wolfram et al.^[17] calculated the volume loss of Q&P-treated 9260 steel with normalized samples with respect to the performance of AR400F samples during dry sand and rubber wheel (DSRW) wear tests, and here also a beneficial effect of austenite was confirmed. Wang et al.^[20] found that by applying a Q&P treatment to a ductile cast iron wear resistance was improved and that the employed partitioning time affected the obtained wear rate, first increasing with the increase of the partitioning time and then decreasing with a further time increasing. Lai et al.^[21] concluded that compared with Q&T treatment, wear resistance of a high C steel was improved by applying a series of Q&PT (quenching and partitioning-tempering) treatments, which was associated with the formation of film-like and blocky austenite during partitioning stage.

In contrast, Haiko et al.^[18] investigated the wear resistance of steels which were directly quenched and partitioned (DQ&P) after thermomechanical rolling and then subjected to impeller-tumbler impact-abrasive wear testing, finding that wear performance depended solely on hardness, regardless of microstructure, and did not see enhancement of wear with increasing RA. The authors argued that the TRIP effect could be detrimental if the matrix cannot accommodate the transformation stresses, providing a pathway for subsurface cracks in the interphase between the martensite matrix and the newly formed untempered one. When analyzing the published data, it is important to consider that the wear resistance of a material depends on various factors such as wear condition, intensity and frequency of load, environment and mechanism, which means that the wear resistance measurements correspond to specific testing conditions, and that a direct comparison cannot be done.

Most of the earlier works characterized the microstructure and wear resistance of different steel grades and compared the wear behavior with that observed in Q&T-treated samples. However, to the best knowledge of the authors, there are no research works that investigate the mechanical stability of the austenite and its transformation into martensite during the wear test. Hence, the current research aims to gain insight into the transformation-induced plasticity phenomenon under wear test conditions and its relationship with wear resistance. In this work, two steels were heat treated by Q&P and the resulting microstructure, hardness, wear resistance, and mechanical stability of austenite phase were characterized. The two steels had a medium and a high C content, which allowed also to analyze the effect of C content.

2. Experimental Section

Two commercial steels were employed, specifically the 41SiNiCrMo7-6 and X100CrMoV8-1-1 steels, hereinafter referred to as medium-C and high-C, respectively. The actual chemical composition of each steel was analyzed by optical emission spectrometry (OES), and it is shown in **Table 1**. These steels

Table 1. Chemical composition of the high-c and medium-c steels (wt%).

Steel grade	C	Si	Mn	Cr	Mo	V	Ni	Al	S	P
High-C	0.92	0.96	0.36	7.9	1.0	1.5	–	–	0.0020	0.020
Medium-C	0.41	1.60	0.83	0.78	0.38	0.06	1.80	0.01	<0.0003	0.008

were selected to be treated by Q&P mainly due to the high Si content and high expected hardenability. In the medium-C steel, the Si content was around the typical content added in Q&P steels to avoid the formation of iron carbides.^[13] It was lower in the high-C steel, although still a certain effect could be expected.^[22] Additionally, the high-C steel contained a significant content of carbides forming elements Cr, Mo, and V, which confer the high hardness and wear resistance properties, and the medium-C steel presented a medium content of Ni, which was expected to contribute to austenite stabilization in the Q&P type thermal treatment.

Phase transformation temperatures (A_{c1} , A_{c3} , M_s , M_f), critical cooling rates (CCR) to avoid diffusion-based phase transformations, and martensitic transformation curves were determined by means of a LINSEIS L78 RITA dilatometer, using cylindrical samples with 3 mm diameter and 10 mm length. First, A_{c1} and A_{c3} temperatures were determined by heating the samples at $10\text{ }^\circ\text{C s}^{-1}$ up to $1100\text{ }^\circ\text{C}$. Then, CCR were determined by heating the samples up to $A_{c3} + 50\text{ }^\circ\text{C}$ and cooling them down to room temperature employing different cooling rates. For the determination of martensitic transformation curves, the samples were heated at $10\text{ }^\circ\text{C s}^{-1}$ $50\text{ }^\circ\text{C}$ above A_{c3} and hold for 120 s. Afterward, samples were cooled down to room temperature by employing a cooling rate of $45\text{ }^\circ\text{C s}^{-1}$ and then were reheated up to $500\text{ }^\circ\text{C}$ at $5\text{ }^\circ\text{C s}^{-1}$. From the resulting dilatometry curves, applying the lever rule between the expansion of the untransformed austenite curve and that from the reheating, martensitic transformation curves were calculated. An additional dilatometry test was carried out, in which samples were directly quenched from $A_{c3} + 50\text{ }^\circ\text{C}$ to measure residual RA in quenched samples. Resulting values of phase transformation temperatures, CCR, and residual austenite contents are summarized in **Table 2**. As can be seen, the CCR were quite low, so undesired transformations during the cooling from $A_{c3} + 50\text{ }^\circ\text{C}$ could be avoided.

Once phase transformation temperatures and CCRs were known, a Q&P cycle was designed for each steel, where a QT corresponding to 20% of untransformed austenite (QT20), a PT of $400\text{ }^\circ\text{C}$ and a Pt of 120 s were considered. The QT20 values were obtained from the martensitic transformation curves determined before (180 and $175\text{ }^\circ\text{C}$ for the high-C and medium-C steels, respectively). The Q&P cycle is represented in **Figure 1**, and cycle parameters are shown in **Table 3**. The Q&P treatments were applied in both steels employing a resistance furnace and

Table 2. Phase transformation temperatures, CCR, and RA of the direct-quenched (DQ) steels.

Steel reference	A_{c1} [$^\circ\text{C}$]	A_{c3} [$^\circ\text{C}$]	M_s [$^\circ\text{C}$]	M_f [$^\circ\text{C}$]	CCR [$^\circ\text{C s}^{-1}$]	RA in DQ samples [%]
High-C	881	987	342	<RT	0.5–1	<5
Medium-C	758	875	270	RT	<2	0

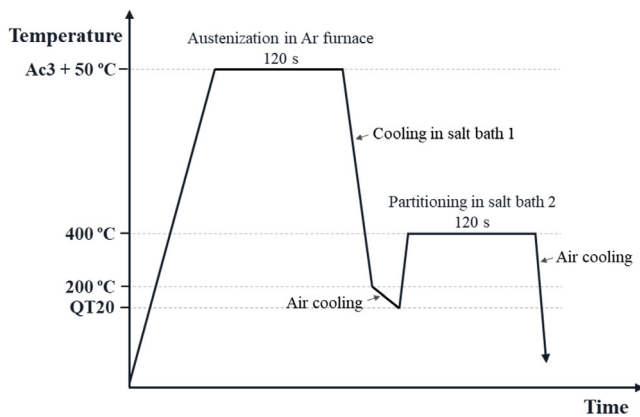


Figure 1. Schematic of the Q&P cycles applied in this work.

Table 3. Q&P cycle parameters.

Steel reference	Heat treatment	Austenization T [°C]/ t [s]	Quenching T [°C]	Partitioning T [°C]/ t [s]
High-C	Q&P	1037/120	180	400/120
Medium-C	Q&P	925/120	175	400/120

two salt baths. First, the samples were fully austenized by heating to $A_{c3} + 50$ °C in an Ar atmosphere furnace. Afterward, the samples were transferred to the first salt bath, with a temperature of 200 °C, to be next cooled in air down to the corresponding QT20, achieving in this way cooling rates above the CCR. Then the samples were transferred into the second salt bath with a temperature of 400 °C to perform the partitioning stage. Finally, the samples were cooled in air to room temperature.

Temperature evolution during the Q&P cycle was monitored by means of two thermocouples, one in the center of the thickness and the other on the surface, observing that the thermal cycle was the same in both positions, which means that thermal heterogeneities did not exist along the thickness of the sample. The monitored Q&P cycles were afterward simulated in the dilatometer in order to better understand the microstructure evolution by analyzing the contraction and expansion occurring along the cycle.

Hardness measurements were carried out in the Q&P-treated samples employing a Vickers Hardness Tester FV-700 model (FUTURE-TECH) using a 10 kg load, applied for 10 s.

The treatments were applied on disks with 6 mm thickness and two different diameters, designed for the subsequent characterization of wear resistance. To characterize the wear resistance of the steels, pin-on-disk (PoD) tests were carried out in a MICROTTEST tribometer, considering a testing configuration where the Q&P-treated samples were the disks. The influence of lineal velocity was tested in the high-C steel by considering two different diameters of the disk. The test parameters are summarized in **Table 4**. After carrying out the test, the volume of wear on the disk was evaluated by measuring a series of wear profiles. The evaluation consisted of making 4 profiles on each of the tracks left in each test, thus obtaining 4 cross-sectional areas. Finally, the specific wear rates (K), in $\text{mm}^3 \text{N}^{-1} \text{m}^{-1}$, of

Table 4. Parameters used for the pin-on-disk tests.

Steel reference	High-C	Medium-C
Test radius [mm]	15 and 45	15
Lineal velocity [cm s^{-1}]	78.3 and 208.3	78.3
Load [N]	20	20
Test duration [min]	122	122
Temperature [°C]	RT	RT
Relative humidity [%]	50	50
Pin material	Al_2O_3	Al_2O_3
Pin diameter [mm]	6	6

the investigated materials were obtained. This operation was carried out using a Dektak 150 Contact Profilometer.

RA content of the Q&P-treated samples was obtained by means of X-ray diffraction (XRD) and according to the ASTM E975–13 standard. XRD patterns were collected by using a Bruker D8 Discover diffractometer equipped with a Cr Twist tube, V filter ($\lambda = 2.291$ Å), PolyCap™ (1 μ single crystal cylinders) system for parallel beam generation (divergence of 0.25°), and a 1-D LynxEye detector (active length in 2θ 2.7°). The samples were mounted on an Eulerian Cradle with automatic controlled X–Y–Z stage. Data were collected from 50 to 120° 2θ (step size = 0.04 and time per step = 1 s). Peak area intensity was evaluated using the peak-fit option of the WinPLOTR software. RA measurements were performed both in the surface of the disks and in the wear tracks. These measurements enabled to evaluate RA content after Q&P treatments (measurements in the surface) and to analyze the mechanical stability of RA under the applied wear test conditions (measurements in the wear track).

Microstructural characterization of the Q&P samples was done by means of a scanning electron microscope (SEM) (QUANTA 200 FEI). A beam voltage of 25 kV and a working distance of 10 mm were employed. In addition, energy-dispersive X-ray spectroscopy (EDS) analysis was carried out in order to identify the composition of some of the constituents. The samples for SEM observation were mechanically polished down to 1 μm and then etched with 2% Nital.

Finally, hardness and wear tests were also performed on Q&T samples of the same steels, following the same testing conditions, and the results were compared with Q&P samples. The tempering conditions followed the guidelines specified for each steel.

3. Results and Discussion

3.1. Dilatometry Curves of the Q&P Heat Treatments

In **Figure 2**, the relative change in length measured in the dilatometry samples subjected to the Q&P cycles monitored in the salt baths is shown for both steels. In the first heating to $A_{c3} + 50$ °C, the austenite formation resulted in the contraction of the sample, whereas the martensite formation in the first cooling to QT20 caused volume expansion. Then, after a second heating to the partitioning temperature, a slight volume expansion

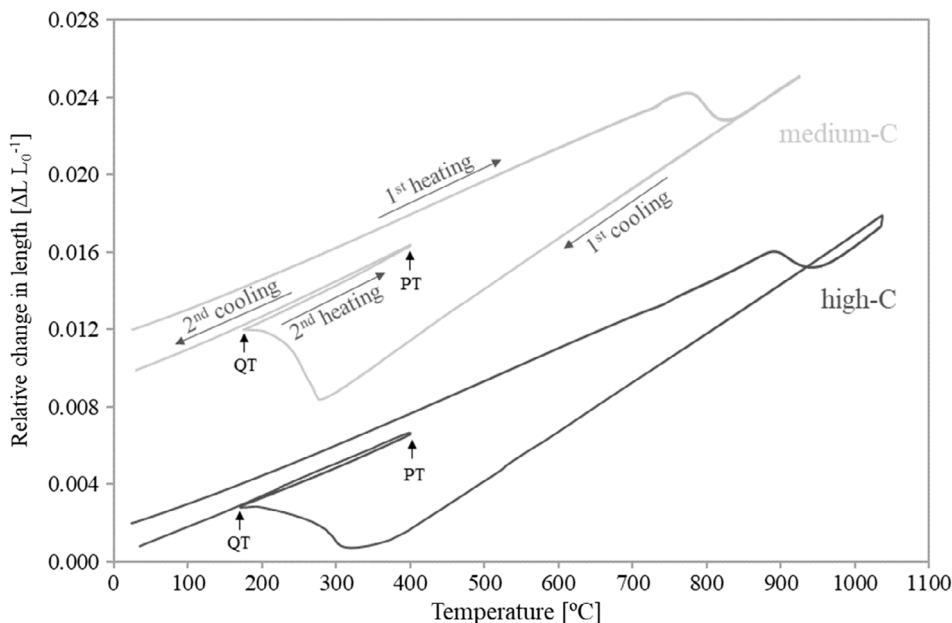


Figure 2. Dilatometry curves of the applied Q&P cycles.

was observed during the holding at the partitioning stage. The latter can be better seen in **Figure 3**, where the relative change in length is represented as a function of the partitioning time. The observed expansion was likely related with C partitioning from the martensite into the austenite.^[23,24] This expansion was rather bigger in the high-C steel, which was likely due to its higher nominal C content. It was therefore to be expected that, for the end of the partitioning, more C had migrated from martensite into austenite in this steel. However, no stabilization of the expansion was observed in either of the steels during the partitioning, which might mean that equilibrium was not reached in the 120 s that took the partitioning step. On the other hand, dilatometry curves during the second cooling to room temperature were analyzed to study the possible formation of secondary martensite. In both steels, the curve was linear and volume change

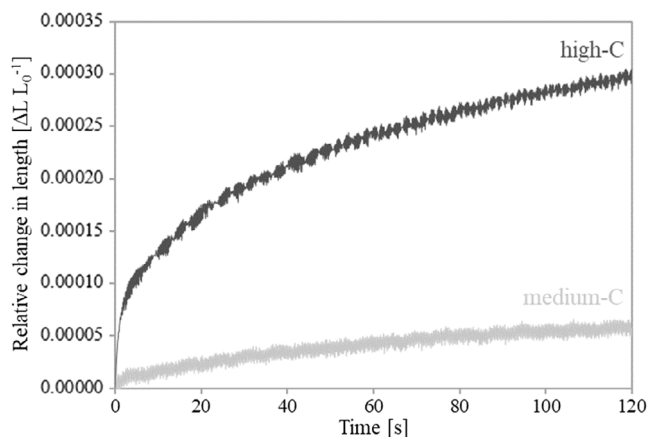


Figure 3. Relative change in length measured during the partitioning stage for the Q&P cycles.

was not observed, which means that the formation of secondary martensite was not significant and, therefore, most of the austenite available at the end of the partitioning was stable enough to be retained in the final microstructure.

3.2. Microstructure

Figure 4 shows an SEM micrograph of the medium-C steel Q&P treated in the salt baths. In the micrograph, bright areas were supposed to be blocky RA and RA laths. As the samples were fully austenized 50 °C above A_{c3} temperature and then the cooling rate was high enough to avoid any transformation before

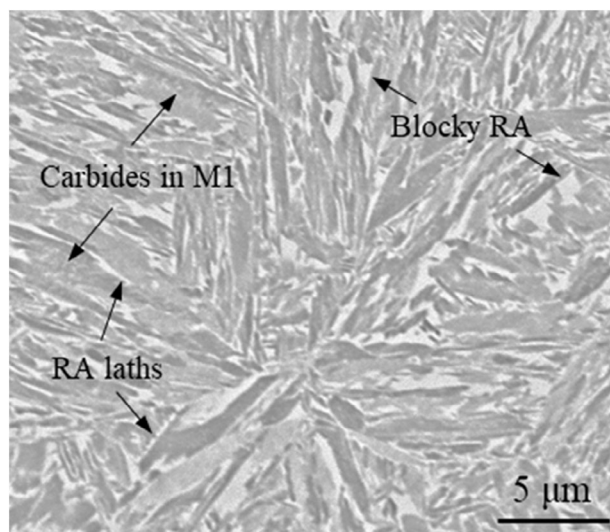


Figure 4. SEM micrograph of the medium-C steel after the Q&P treatment.

achieving QT20, ferrite was not expected to be found in the microstructure. Therefore, the gray areas observed in Figure 4 are supposed to be tempered martensite (M1) with some little and fine carbide precipitation inside^[25] could be observed. The austenite content measured by XRD was $20 \pm 1\%$, which means that the total amount of austenite existing at QT20 was retained in the final microstructure. It reveals that no competitive reactions occurred in the partitioning stage and that austenite existing at the end of the partitioning was stable enough to be completely retained, which is in agreement with the dilatometry curves shown before. Additionally, the austenite content measured in the directly quenched sample was less than 5% (Table 2), which means that the Q&P heat treatment was suitable to retain a significant amount of austenite in the final microstructure.

In the case of the high-C steel, the microstructure after Q&P treatment (Figure 5a,b) showed distinctive features. Although tempered martensite and austenite laths can be also found, here the presence of carbides was more notable. Furthermore,

carbides showed different size, morphology, and chemical composition. On the one hand, fine carbides with globular morphology (point x2 in Figure 5a) and containing V, Cr, and a small amount of Mo were observed and analyzed (Figure 5d). On the other hand, very coarse phases with irregular shape were also observed (points x3 and x4 in Figure 5b), which based on the EDS analysis (Figure 5e,f) were also supposed to be carbides containing Cr, V, and Mo. Finally, as it can be seen in the EDS analysis (Figure 5c) of the matrix (point x1 in Figure 5a), Mo and V peaks showed lower intensity than in the carbides.

The RA measured by XRD in the high-C steel after the Q&P treatment was $22 \pm 1.1\%$, which again means that the thermal cycle was appropriate to stabilize all the austenite. In this case, the austenite content measured in the final microstructure was slightly higher than the austenite content existing at QT, which was supposed to be 20%. The slight increase can be explained based on the following observations: 1) QT20 temperature was determined from martensitic transformation curves obtained by dilatometry, where the cooling rate applied in the quenching

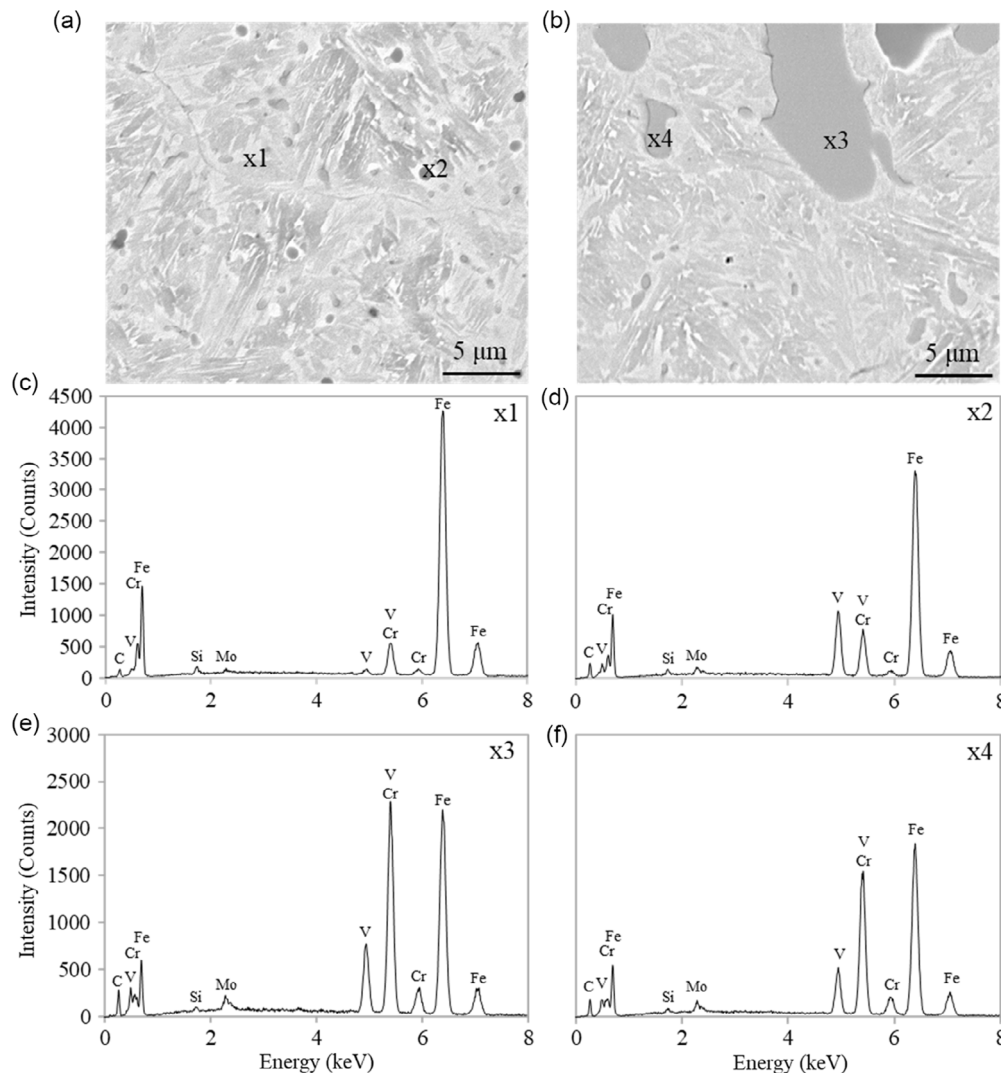


Figure 5. SEM micrographs a,b) and EDS analysis c–f) of the high-C steel after the Q&P treatment.

was not exactly the same as the one obtained in the salt bath. The cooling rate can affect the martensite transformation curve,^[26] and, therefore, the austenite content existing at QT20 in the salt bath samples might have been slightly higher, resulting in a final austenite content above the defined 20% and 2) in steels with high C content treated by Q&P, a displacement of the interface toward martensite has been reported, thus achieving values of RA higher than those of the QT.^[27]

Thermo-Calc calculations were performed to better understand the carbides present in both steels. The results are shown in **Figure 6**. As it can be seen in Figure 6a, the main precipitated phase in the medium-C steel was cementite; therefore, the carbides observed inside the tempered martensite in Figure 4 were likely this phase. In the high-C steel up to around 10% of the M7C3 and M23C6 phases can be expected in the microstructure according to Thermo-Calc (Figure 6b), being M = Fe, Cr, V, or Mo. The composition of each phase as a function of temperature is shown in Figure 6c,d. Both phases contain a high content of Cr, but only the M7C3 phase contain a relatively high V content.

Besides, the M23C6 phase shows a considerable Mo content, which was barely detected by EDS analysis performed in the high-C steel. Therefore, it can be said that the phases analyzed in Figure 5a,b (points x2, x3 and x4) might be M7C3, although further research would be needed to better determine the type of carbide. According to Thermo-Calc, the dissolution temperature of the M7C3 phase (≈ 1220 °C) is significantly higher than the austenization temperature employed in the Q&P treatments (1037 °C), which means that likely these carbides were eutectic carbides present in the initial microstructure or precipitated during austenization and were not significantly affected by the Q&P heat treatment.^[28,29] In cast irons with elevated contents of Cr, eutectic M7C3 carbides tend to transform into M23C6 carbides. However, when Cr content was below 10–25 wt%, M7C3 carbides do not appear to undergo any structural changes.^[29] On the other hand, the austenization and subsequent quenching might lead to a formation of secondary spheroid M7C3 particles (point x2 in Figure 5a) within the primary austenitic phase.^[30]

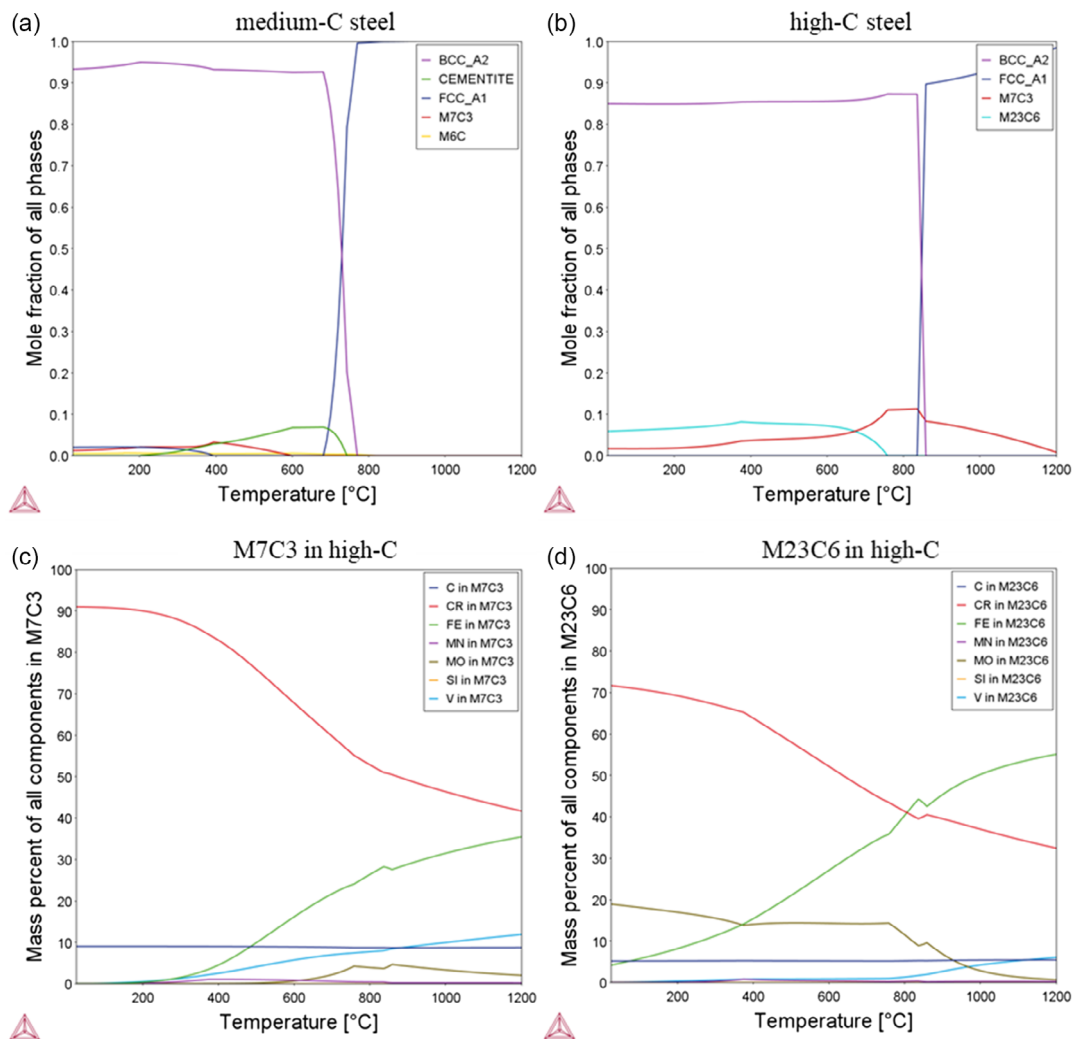


Figure 6. Phase fraction as a function of temperature of a) the high-C and b) medium-C steels, and composition of the high-C steel's c) M7C3 and d) M23C6 phases obtained by Thermo-Calc calculations.

3.3. Hardness

Hardness measurements were performed in the Q&T- and Q&P-treated samples in both steels. The average values obtained after five indentations are shown in **Figure 7**. The Q&P treatment resulted in a considerably lower hardness, especially in the high-C steel. The high-C steel contained relatively high contents of carbides forming elements like Cr (7.9 wt%), V (1.5 wt%), and Mo (1 wt%). Thus, in the tempering, apart from eliminating the stresses generated during the martensitic transformation and soften the structure restoring the toughness of the material, secondary precipitation hardening can be achieved.^[31–33] As it was seen in **Figure 5**, Cr-, V-, and Mo-containing carbides were visible in the microstructure of the Q&P-treated high-C steel. However, the total amount of carbides was likely lower than in the Q&T steel, as the partitioning temperature was below the tempering temperature applied in the high C steel (around 500 °C), which aimed to obtain the maximum secondary hardening of carbides. Furthermore, the Q&P steel contained C-enriched RA which likely lowered the overall hardness value.^[34]

In the medium-C steel, Q&P treatment resulted in lower hardness as well, although the decrease was less significant in comparison with the high-C steel. Unlike in the high-C steel, tempering treatment was only applied to eliminate residual stresses produced during the quenching and restore the toughness.^[12,35] Thus, less differences were expected from the point of view of the contribution of carbides to the hardness among Q&T and Q&P samples. Consequently, the lower hardness in Q&P sample could be mainly the consequence of a higher amount of C-enriched austenite which left less C available for the tempered martensite.^[36]

3.4. Wear Behavior

Wear rates were calculated from the pin-on-disk tests for both steels and both Q&P and Q&T treatments. **Figure 8** shows the influence of the heat treatment in both steels and the influence of the testing linear velocity in the Q&P-treated high-C steel on the wear rate. When comparing the influence of the heat treatment (**Figure 8a,b**), the difference in the wear rate was

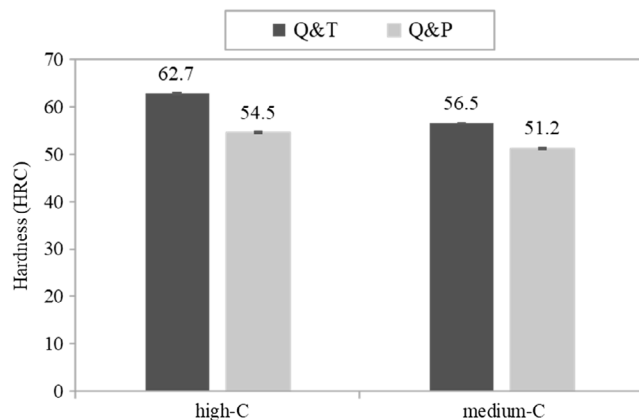


Figure 7. Hardness values measured in the high-C and medium-C steels after the application of Q&T or Q&P heat treatments.

insignificant both in the high-C and the medium-C steel. However, it was shown before that the difference in hardness between the Q&P and Q&T-treated steels was considerably high, especially in the high-C steel. Thus, Q&P-treated samples showed a significantly lower hardness but the same wear resistance than Q&T samples. This behavior demonstrates that hardness was not the only parameter affecting the wear resistance and that the RA may play a key role.^[15] On the other hand, when analyzing the influence of the testing linear velocity in the Q&P-treated high-C steel (**Figure 8c**), it can be seen that it is also insignificant.

It is difficult to compare the results obtained in this work with those reported in the literature. On the one hand, there is very little literature studying the wear resistance of Q&P-treated steels, and even less studying the wear behavior through unidirectional sliding tests, as in the present work. On the other hand, the results obtained from PoD tests strongly depend on the testing conditions. However, most of the results reported in the literature show an improvement in the wear resistance by the application of Q&P heat treatments as mentioned in the introduction part of this work.

In the present work, wear resistance was not improved by the substitution of the Q&T by Q&P treatment. However, only one Q&P condition was studied, and it is possible that the optimization of the Q&P cycle parameters could result in an improvement. The application of Q&PT treatments could also be beneficial for the high-C steel. Additionally, different PoD testing conditions could also result in a different behavior. Nevertheless, the results showed similar wear rates after both treatments with significantly lower hardness after Q&P. The reduced hardness could be related with an improvement of other properties typically required in this type of steels, such as toughness, although it would need to be further investigated.

3.5. Retained Austenite Stability

The austenite transformation into martensite is thought to be responsible for enhancing the wear behavior in Q&P steels.^[15] With the aim of assessing austenite stability and its potential transformation into martensite during the wear test, RA content was measured in the wear track of the PoD-tested disks and compared with RA contents measured before in the surface of the disks. In **Figure 9**, these results are shown for both steels and different linear velocity conditions employed (the latter only for the high-C steel).

In the high-C steel and the lower linear velocity condition, austenite transformation was not observed. The higher linear velocity condition resulted in the transformation of a significant part of the initial RA content. Therefore, it can be said that under the test conditions employed in this work, the mechanical stability of austenite against transformation in this steel was too high and the wear behavior of the material did not benefit from transformation hardening. It is known that the C content is the main factor affecting RA stability.^[37–39] In the high-C steel, the C content was high (0.92%), and it is likely that, in spite of the high fraction of carbides present in the microstructure, the C content in the RA after the Q&P treatment was too high to allow martensite transformation in the employed testing conditions.

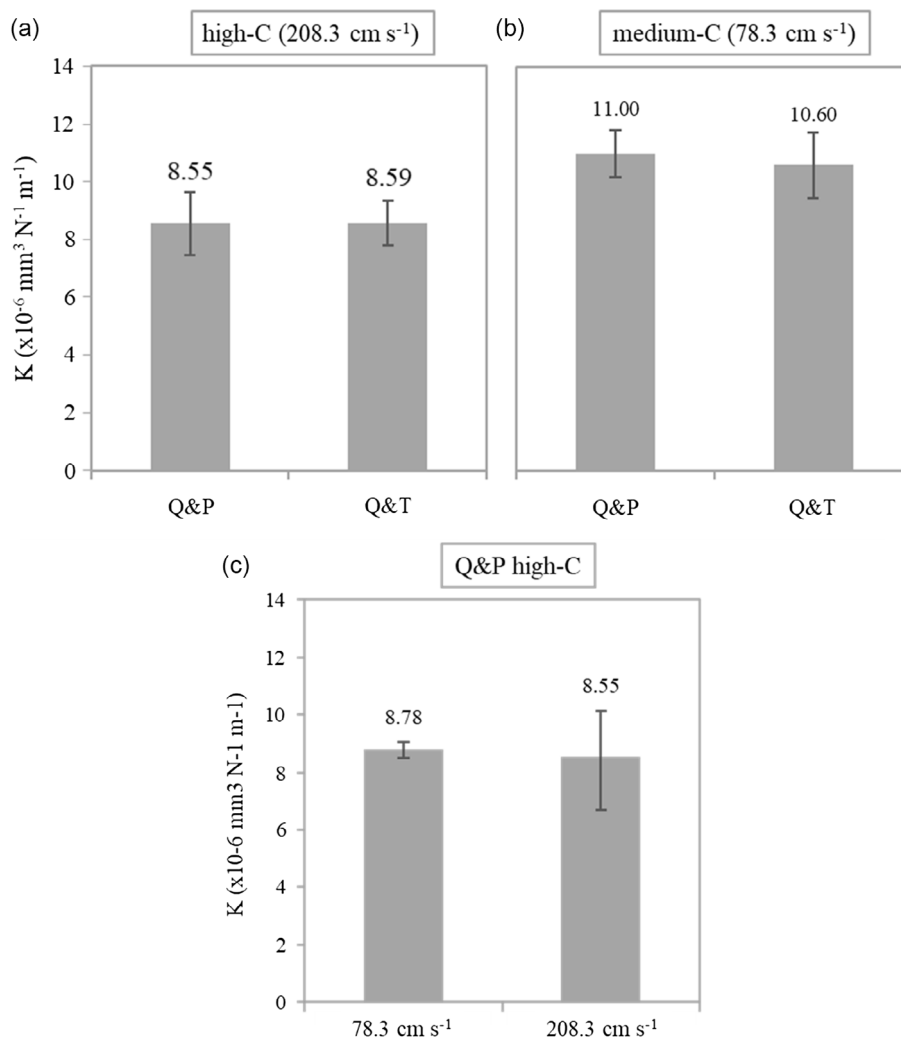


Figure 8. Wear rate (K [$\text{mm}^3 \text{N}^{-1} \text{m}^{-1}$]) calculated from the PoD tests. Comparison between Q&P and Q&T-treated high-C a) and medium-C b) steels and comparison between Q&P-treated high-C steel tested with different linear velocity c).

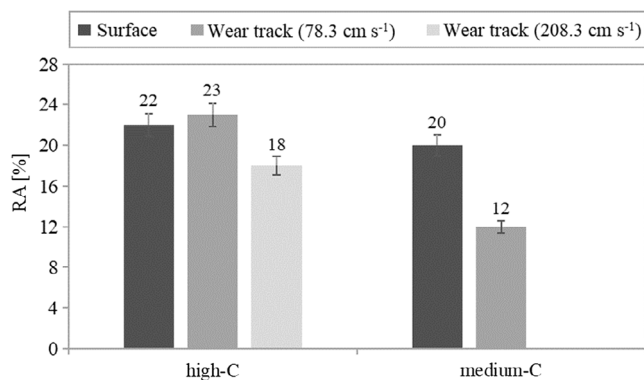


Figure 9. RA content measured in the surface and the wear track of the pin on disk-tested disks, under 208.3 cm s⁻¹ linear velocity condition in the high-C and medium-C steels and, also, under 78.3 cm s⁻¹ linear velocity condition in the high-C steel.

In the medium-C steel, a higher amount of the austenite transformed during the tests, specifically 40% of the initial RA. This steel contains a lower C content (0.41%), which might result in a lower C content in RA after Q&P treatment than in the high-C steel and, consequently, in a higher transformation into austenite. However, this transformation seemed to be still low to result in an improvement of wear resistance behavior of Q&P-treated steel with regard to the Q&T-treated sample.

Apart from the C content, it is known that other factors can affect the stability of austenite. It has been reported that film-like RA can be mechanically more stable in martensitic microstructures than blocky RA, suggesting that this stability may be due to surrounding martensite laths suppressing the transformation of film-like RA.^[39–42] In the SEM image of the medium-C steel (Figure 4), some areas with blocky austenite were observed, whereas in the high-C steel (Figure 5) austenite laths predominated, which could also contribute to the higher austenite stability of the high-C steel. Furthermore, in the case of the

high-C steel, a stronger matrix could lead to an increase in the mechanical stability of RA and sometimes this makes the transformation of RA to martensite not to occur even under the actions of stress or strain.^[43]

Received: January 30, 2023
Revised: March 27, 2023
Published online: April 27, 2023

4. Conclusion

In this work, the microstructure, hardness, and wear resistance of a medium and a high C steels heat treated by Q&P treatment were studied. The measured hardness and wear rates were compared with those shown by the same steels heat treated by Q&T treatment. The conclusions drawn were the following: 1) Q&P treatments were effective in stabilizing the austenite content existing at QT, giving rise to a final microstructure containing tempered martensite and around 20% RA in both steels. Precipitation of Cr, V, and Mo carbides was also observed in Q&P treated high-C steel. 2) After the application of the Q&P treatment, the wear rate values obtained in both steels were similar to those obtained after the Q&T treatment. However, the hardness values of the Q&P-treated samples were considerably lower than those of the Q&T-treated samples, which means that hardness was not the only parameter influencing the wear resistance. 3) In the high-C steel, the austenite content transformed into martensite during the wear tests was low, which revealed a high mechanical stability of austenite phase in the applied wear test conditions. Therefore, austenite transformation phenomenon scarcely contributed to the attained wear resistance. The higher mechanical stability of austenite in the high-C steel could be related with its higher C content, although other factors, such as austenite morphology and matrix strength, could also affect. 4) In the medium-C steel, a higher content of austenite transformed during the test, and this transformation seemed be enough to compensate the hardness loss and provide a similar wear resistance in comparison with Q&T samples.

Acknowledgements

This research is partially funded by the Basque Government in the CHALET project, which has received funding from the HAZITEK Program under grant agreement ZL-2020/00434. The authors thank for technical and human support provided by SGIker (UPV/EHU/ERDF, EU).

Conflict of Interest

The authors declare no conflict of interest.

Data Availability Statement

Research data are not shared.

Keywords

austenite stability, medium and high C steels, quenching and partitioning, wear behavior

- [1] T. Liu, M. T. Kiser, T. E. Clements, in *Int. Symp. Recent Developments in Plate Steels*, Winter Park, CO **2011**, pp. 71–80.
- [2] J. A. Hawk, R. D. Wilson, D. R. Danis, M. T. Kiser, *ASM Handbooks, Failure Analysis and Prevention*, Vol. 906–921, ASM International, Materials Park, OH **2003**, p. 11.
- [3] M. J. Pérez, M. M. Cisneros, H. F. López, *Wear* **2006**, *260*, 879.
- [4] O. Haiko, I. Miettunen, D. Porter, N. Ojala, V. Ratia, V. Heino, A. Kemppainen, *Tribologia* **2017**, *35*, 5.
- [5] J. J. Coronado, A. Sinatora, *Wear* **2009**, *267*, 2077.
- [6] L. C. Cheng, T. B. Wu, C. T. Hu, *J. Mater. Sci.* **1988**, *23*, 1610.
- [7] T. Jian-Min, Z. Yi-Zhong, S. Tian-Yi, D. Hai-Jin, *Wear* **1990**, *135*, 217.
- [8] N. Maheswari, S. G. Chowdhury, K. C. Hari Kumar, S. Sankaran, *Mater. Sci. Eng., A* **2014**, *600*, 12.
- [9] T. Tsuchiyama, T. Sakamoto, S. Tanaka, T. Masumura, *ISIJ Int.* **2020**, *60*, 2954.
- [10] S. G. Liu, S. S. Dong, F. Yang, L. Li, B. Hu, F. H. Xiao, Q. Chen, H. S. Liu, *Mater. Des.* **2014**, *56*, 37.
- [11] J. Speer, D. K. Matlock, B. C. De Cooman, J. G. Schroth, *Acta Mater.* **2003**, *51*, 2611.
- [12] N. Fonstein, *Advanced High Strength Sheet Steels*, Springer, Cham **2015**, <https://doi.org/10.1007/978-3-319-19165-2>.
- [13] A. M. Streicher, J. G. Speer, D. K. Matlock, B. C. De Cooman, in *Int. Conf. Advances High Strength Sheet Steels for Automotive Applications - Proc.*, Winter Park, CO **2004**, p. 51.
- [14] J. G. Speer, E. De Moor, K. O. Findley, D. K. Matlock, B. C. De Cooman, D. V. Edmonds, *Metall. Mater. Trans. A* **2011**, *42*, 3591.
- [15] H. Y. Dong, K. M. Wu, X. L. Wang, T. P. Hou, R. Yan, *Wear* **2018**, *402–403*, 21.
- [16] K. Wasiak, E. Skoček, W. A. Świątnicki, in *METAL 2014 - 23rd Int. Conf. Metallurgy and Materials, Conf. Proc.*, Brno, Czech Republic, EU **2014**.
- [17] P. Wolfram, C. Hensley, R. Youngblood, R. Stewart, E. de Moor, J. G. Speer, *Mater. Sci. Forum* **2018**, *941*, 568.
- [18] O. Haiko, M. Somani, D. Porter, P. Kantanen, J. Kömi, N. Ojala, V. Heino, *Wear* **2018**, *400–401*, 21.
- [19] P. V. Moghaddam, J. Hardell, E. Vuorinen, B. Prakash, *Wear* **2019**, *428–429*, 193.
- [20] Z. Wang, B. Huang, H. Chen, C. Wang, J. Ma, X. Zhao, *J. Mater. Eng. Perform.* **2020**, *29*, 4370.
- [21] J. Ping Lai, L. Ping Zhang, W. Gong, X. Xu, C. An Xiao, *Wear* **2019**, *440–441*, 203096.
- [22] B. M. Linke, T. Gerber, A. Hatscher, I. Salvatori, I. Aranguren, M. Arribas, *Metall. Mater. Trans. A* **2018**, *49*, 54.
- [23] M. J. Santofimia, L. Zhao, R. Petrov, C. Kwakernaak, W. G. Sloof, J. Sietsma, *Acta Mater.* **2011**, *59*, 6059.
- [24] M. J. Santofimia, L. Zhao, J. Sietsma, *Mater. Sci. Forum* **2012**, *706*, 2290.
- [25] D. V. Edmonds, K. He, F. C. Rizzo, B. C. De Cooman, D. K. Matlock, J. G. Speer, *Mater. Sci. Eng., A* **2006**, *438–440*, 25.
- [26] S. Pang, G. Wu, W. Liu, M. Sun, Y. Zhang, Z. Liu, W. Ding, *Mater. Sci. Eng., A* **2013**, *562*, 152.
- [27] N. Zhong, X. Wang, Y. Rong, L. Wang, *J. Mater. Sci. Technol.* **2006**, *22*, 751.
- [28] S. K. Hann, J. D. Gates, J. V. Be, *J. Mater. Sci.* **1997**, *32*, 3443.
- [29] A. Wiengmoon, T. Chairuangri, A. Brown, R. Brydson, D. V. Edmonds, J. T. H. Pearce, *Acta Mater.* **2005**, *53*, 4143.
- [30] A. E. Karantzalis, A. Lekatou, H. Mavros, *J. Mater. Eng. Perform.* **2008**, *18*, 174.

- [31] N. Zhong, X. D. Wang, L. Wang, Y. H. Rong, *Mater. Sci. Eng., A* **2009**, 506, 111.
- [32] S. Zhou, K. Zhang, Y. Wang, J. F. Gu, Y. H. Rong, *Mater. Sci. Eng., A* **2011**, 528, 8006.
- [33] S. Zhou, K. Zhang, N. Chen, J. Gu, Y. Rong, *ISIJ Int.* **2011**, 51, 1688.
- [34] P. J. Jacques, Q. Furnémont, F. Lani, T. Pardoën, F. Delannay, *Acta Mater.* **2007**, 55, 3681.
- [35] V. I. Zurnadzhy, V. G. Efremenko, K. M. Wu, A. Y. Azarkhov, Y. G. Chabak, V. L. Greshta, O. B. Isayev, M. V. Pomazkov, *Mater. Sci. Eng., A* **2019**, 745, 307.
- [36] X. Yan, J. Hu, X. Zhang, W. Xu, *Tribol. Int.* **2022**, 175, 107803.
- [37] A. M. Gola, M. Ghadamgahi, S. W. Ooi, *Wear* **2017**, 376–377, 975.
- [38] S. Hernandez, A. Leiro, M. R. Ripoll, E. Vuorinen, K. G. Sundin, B. Prakash, *Wear* **2016**, 360–361, 21.
- [39] X. C. Xiong, B. Chen, M. X. Huang, J. F. Wang, L. Wang, *Scr. Mater.* **2013**, 68, 321.
- [40] F. Hu, K. M. Wu, T. P. Hou, A. A. Shirzadi, *Mater. Sci. Technol.* **2013**, 29, 947.
- [41] F. Hu, K. M. Wu, P. D. Hodgson, *Mater. Sci. Technol.* **2016**, 32, 40.
- [42] Z. Zhu, Y. Liang, C. Yin, X. Ren, M. Yang, J. Zou, *Appl. Surf. Sci.* **2022**, 595, 153548.
- [43] B. Liu, W. Li, X. Lu, X. Jia, X. Jin, *Wear* **2019**, 428–429, 127.